Journal of Civil Engineering and Urban Planning (2026)
Clausius Scientific Press, Canada

DOI: 10.23977/jceup.2026.080104
ISSN 2616-3969 Vol. 8 Num. 1

Research on Corrosion Damage Assessment of Cable Stays Based on Eddy Current Testing

Jiawei Liu, Yingchun Chen

Beijing University of Technology, Beijing, China

Keywords: Cable-Stayed Bridge; Corrosion Damage; Eddy Current Testing; Detection Signal; Lightweight Differential Sensor

Abstract: The detection of corrosion damage in cable-stayed bridges is a critical issue in engineering practice. This study systematically investigates this problem, employing a lightweight differential electromagnetic sensor based on eddy current testing principles as the core detection device. A simulation and experimental protocol for corrosion detection of cable-stayed bridges is developed. Pitting corrosion specimens are prepared through mechanical cutting, while uniform corrosion specimens are fabricated via electrochemical etching, providing a reliable specimen foundation for subsequent experiments. The feasibility of detecting corrosion damage in cable-stayed bridges using the lightweight differential electromagnetic sensor is validated through simulation models. Furthermore, the influence of corrosion severity and damage width on detection signals is explored. Experimental analysis confirms the sensor's capability to detect both pitting and uniform corrosion specimens, with experimental results showing excellent agreement with simulation predictions. These findings offer theoretical support and technical references for engineering detection of corrosion damage in cable-stayed bridges.

1. Introduction

With the continuous growth of social economy, the construction of transportation infrastructure has achieved leapfrog development. Tied bridges have been widely adopted due to their aesthetic design, rational structure, and moderate construction costs [1-3].Under sudden temperature changes and rain erosion, the PE sheath of cable-stayed bridges is highly susceptible to cracking, leading to internal corrosion [7-9] and consequently reduced load-bearing capacity. It affects the health status of cable-stayed bridges, and in severe cases may even lead to irreversible major safety accidents with substantial economic losses [10-11].Therefore, the detection of cable corrosion damage is of great engineering significance, and its detection and evaluation has become a key research focus in the field of structural non-destructive testing [4-6,12-13].

Djeddi et al. [14] utilized acoustic emission technology to detect and monitor the corrosion evolution process of steel strands, thereby validating the feasibility of acoustic emission technology for corrosion detection and assessment in steel strands. Vanniamparambil et al. [15] integrated digital image processing with acoustic emission technology to detect wire corrosion fractures, providing a more intuitive assessment of damage conditions.Zhang et al. [16] employed ultrasonic guided wave detection to acquire the original ultrasonic guided wave signals of corrosion defects,

and utilized signal processing techniques to achieve the localization of these defects. Zitoun et al. [18] proposed improving the accuracy of magnetostrictive guided wave detection for corrosion damage by adjusting the direction and magnitude of both static and dynamic magnetic fields. Wu et al. [19] proposed a novel magnetic flux leakage detection method, which improved the accuracy of circumferential corrosion damage detection.[17]

Significant research progress has been made globally in the field of cable-stayed bridge corrosion damage detection, yet studies utilizing eddy current testing principles for corrosion assessment remain relatively scarce. This study systematically investigates corrosion damage detection in cable-stayed bridges by employing lightweight differential electromagnetic sensors based on eddy current principles. Experimental protocols were designed to prepare pitting and uniform corrosion specimens, while simulation models were established to analyze the impact of corrosion width and severity on detection signals. Experimental validation confirmed the feasibility of lightweight differential electromagnetic sensors for corrosion detection, with simulation results being cross-checked. These findings provide theoretical foundations for corrosion damage assessment and facilitate the practical application of this technology in engineering projects.

2. Detection Principle and Experimental Scheme

2.1 Detection Principle

Eddy current testing is based on the principle of electromagnetic induction. When an alternating current is applied to the excitation coil, eddy currents are generated on the surface of the conductive specimen. The presence of defects in the specimen causes distortion of these eddy currents, leading to changes in the magnetic field. Damage assessment and localization are achieved by detecting these magnetic field variations.

This principle boasts advantages such as high precision, high efficiency, and rapid detection, making it widely applicable in the field of cable-stayed bridge damage inspection with strong engineering application prospects. Therefore, this study conducts systematic investigations based on eddy current testing methods.

2.2 Experimental Design

This experiment utilizes an independently developed cable-stayed cable non-destructive testing system, employing a three-axis transmission test bench to enable uniform sensor scanning of the cables. The system comprises a lightweight differential electromagnetic sensor, excitation module, electromagnetic signal acquisition module, data processing module, and data analysis module. The lightweight differential electromagnetic sensor adopts a dual-ended differential excitation configuration with central signal reception, where both the excitation and reception components utilize single-turn coils. The excitation module, electromagnetic signal acquisition module, and data processing module are integrated into a single microcontroller.

The test specimens consist of inclined cables composed of seven steel wires with a diameter of 5mm. To accurately simulate real-world engineering conditions, two types of corrosion specimens were fabricated: the first is a uniformly corroded inclined cable, where all wires except the central one exhibit full-section corrosion; the second is a pitting corrosion inclined cable, with only a single wire undergoing pitting corrosion. The wire bundles are secured using PVC insulated tape and externally wrapped with a 2mm-thick poly(methyl methacrylate) tube as the cable protective sheath. The appearance of the corroded inclined cable is illustrated in Figure 1.

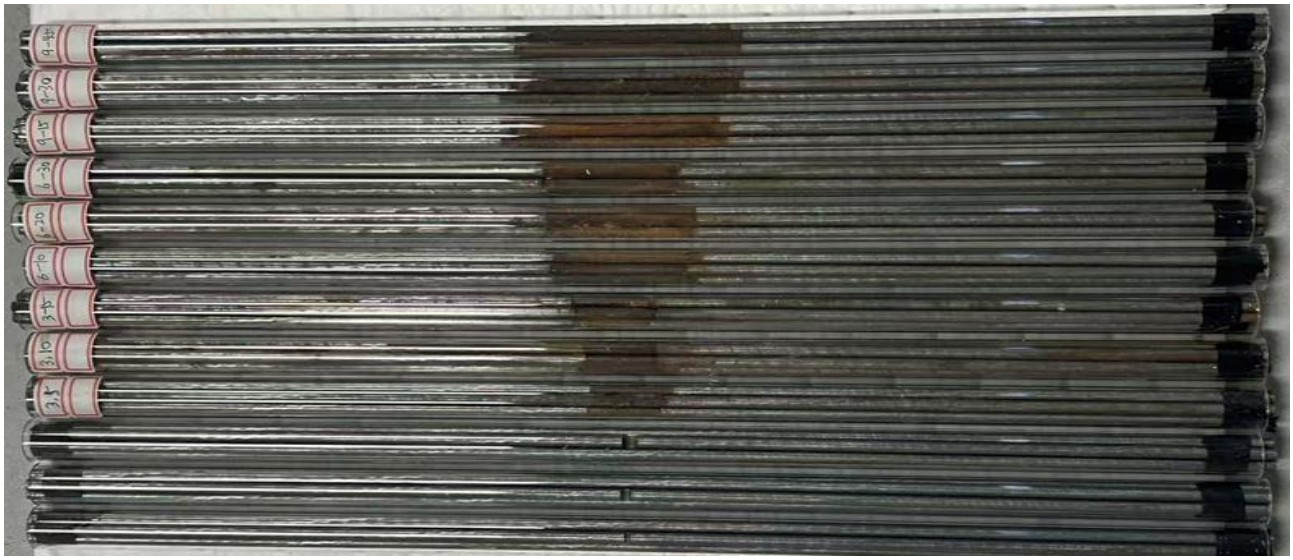

Figure 1. Appearance of corroded stay cable

2.3 Pitting Test Specimen Preparation

This experiment focused on preparing pitting-damaged steel wires using high-strength galvanized steel wires with a diameter of 5 mm and ultimate tensile strength of 1770 MPa. The notch shape was designed as hemispherical, with three notch depths (d) sequentially set at 1 mm, 2 mm, and 3 mm, and three notch lengths (L) sequentially set at 2 mm, 4 mm, and 6 mm. The schematic diagram of pitting damage is shown in Figure 2.

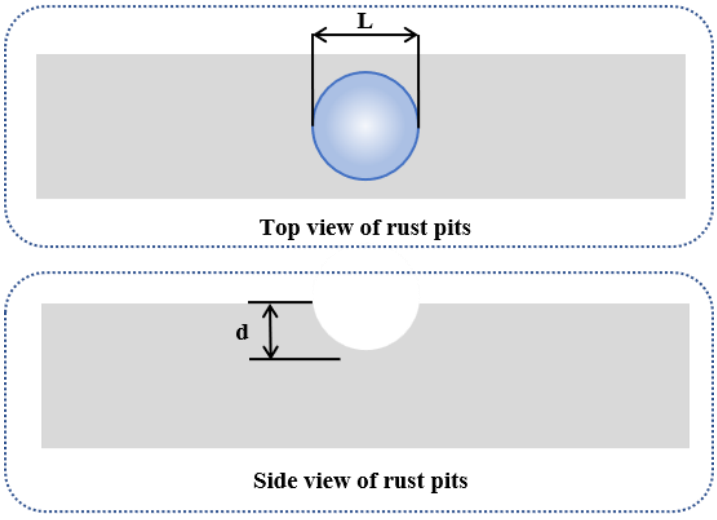

Figure 2: Schematic diagram of pitting corrosion damage

The steel wire had a length of 50 cm, with the pitting corrosion center located at the midpoint along its longitudinal axis. Mechanical cutting was employed to create pitting corrosion damage, ensuring that the shape and size of the damage strictly met the experimental requirements. A local view of the pitting corrosion damage is shown in Figure 3.

Figure 3: Local view of pitting corrosion damage

2.4 Preparation of Uniform Corrosion Specimens

To improve the fabrication efficiency of uniform corrosion specimens and maximize the simulation of real corrosion, this study independently designed and fabricated an electrochemical accelerated corrosion device, as shown in Figure 4. The experimental apparatus consists of four components: an electrolytic cell, a DC voltage stabilizer power supply, electrolyte, and electrodes.

The electrolytic cell features a multi-compartment structure designed for series electrolysis of eight steel wires, significantly enhancing corrosion treatment efficiency. By maintaining a uniform electrolytic environment, it ensures consistent corrosion levels across batches of steel wires, saving time and improving overall efficiency. Acrylic material is used to prevent chemical reactions during electrolysis while ensuring durability and structural strength. Precision machining techniques minimize processing errors, providing hardware assurance for producing uniformly corroded test specimens.

The DC regulated power supply features a dual-channel independent power source (32V/6A) capable of delivering stable constant current excitation. It incorporates a high-current protection design to ensure experimental safety while providing excitation. The 32V voltage meets most electrolysis requirements, while the 6A current accommodates varying electrolysis intensities, further guaranteeing smooth electrolysis processes.

The electrolyte employs a 10% sodium chloride solution, providing high concentrations of sodium and chloride ions to significantly enhance solution conductivity, thereby achieving simulation of real-world environments and ensuring authentic corrosion behavior. This electrolyte offers advantages such as easy preparation, low cost, low corrosiveness to electrolyzers and electrodes, and excellent applicability.

Carbon rods were selected as auxiliary electrodes due to their excellent corrosion resistance, conductivity, and stability. Additionally, the material cost is relatively low, which reduces experimental expenses and meets the requirements of the experiment.

When fabricating corrosion specimens, waterproof adhesive is first applied to encapsulate specific sections of the steel wire to control corrosion extent. The encapsulated wires are then sequentially inserted into the electrolytic cell and connected in series with carbon rods. The power supply's positive terminal is connected to the steel wire while the negative terminal links to the carbon rod. The corrosion intensity of the steel wire is precisely regulated by adjusting the DC current level and excitation duration.

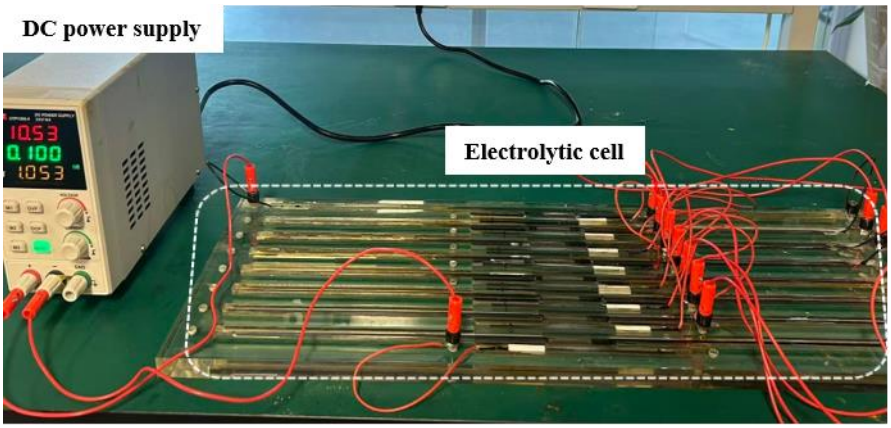

(a) overall setup diagram

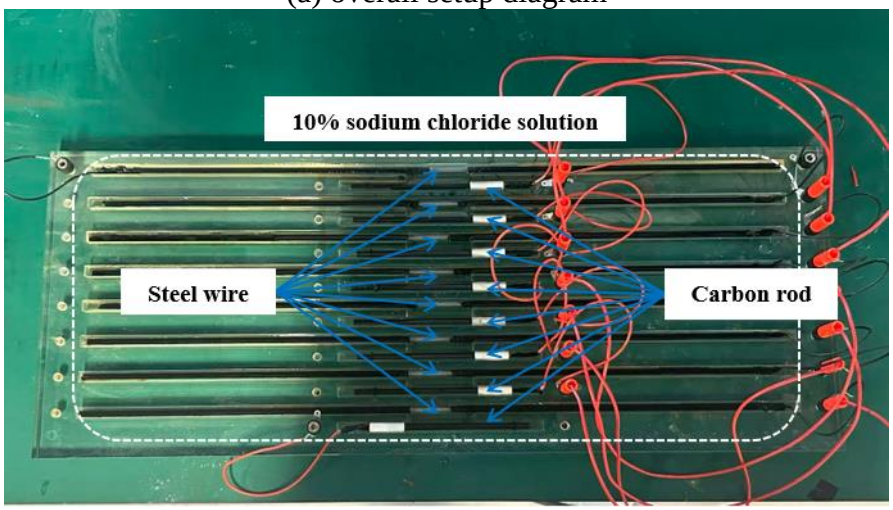

(b) electrolytic cell

Figure 4. Diagram of electrochemical corrosion apparatus

When the electrolyte current remains constant, the electrolysis time is directly proportional to the corrosion extent per unit length of steel wire. This experiment achieves precise control over both corrosion severity and width by regulating electrolysis duration and preset exposed wire width. The specific parameter design includes three target corrosion widths (3 cm, 6 cm, and 9 cm) corresponding to specimens labeled C3, C6, and C9 respectively. Electrolysis durations are set as follows: 5 h, 10 h, and 15 h for C3 specimens; 10 h, 20 h, and 30 h for C6 specimens; and 15 h, 30 h, and 45 h for C9 specimens.

The quality and metal loss rate testing methods are as follows: High-precision electronic balances were used to measure the initial mass of each specimen before corrosion and the residual mass after corrosion. Parallel tests were conducted for each working condition, with the mass average value calculated. Assuming uniform corrosion extent in the wire's corroded area, the metal loss rate for individual specimens was calculated using the formula "(post-corrosion mass-pre-corrosion mass) / original mass of the corroded area × 100%". The final value was determined by averaging the calculated results under identical working conditions. Specific corrosion severity levels are shown in Table 1. The visual appearance and corrosion morphology of wire specimens under various corrosion conditions are illustrated in Figure 5.

Table 1: Corrosion degree of steel wire

Specimen number	Corrosion time (h)	Mass before corrosion (g)	Mass after corrosion (g)	Section metal loss rate at corroded area (%)
C3	5	78.06g	77.58g	10.2%
	10		77.14g	19.2%
	15		76.72g	28.6%
C6	10	78.04g	77.13g	9.7%
	20		76.23g	19.3%
	30		75.46g	27.6%
C9	15	78.07g	76.58g	10.6%
	30		75.31g	19.3%
	45		74.02g	28.8%

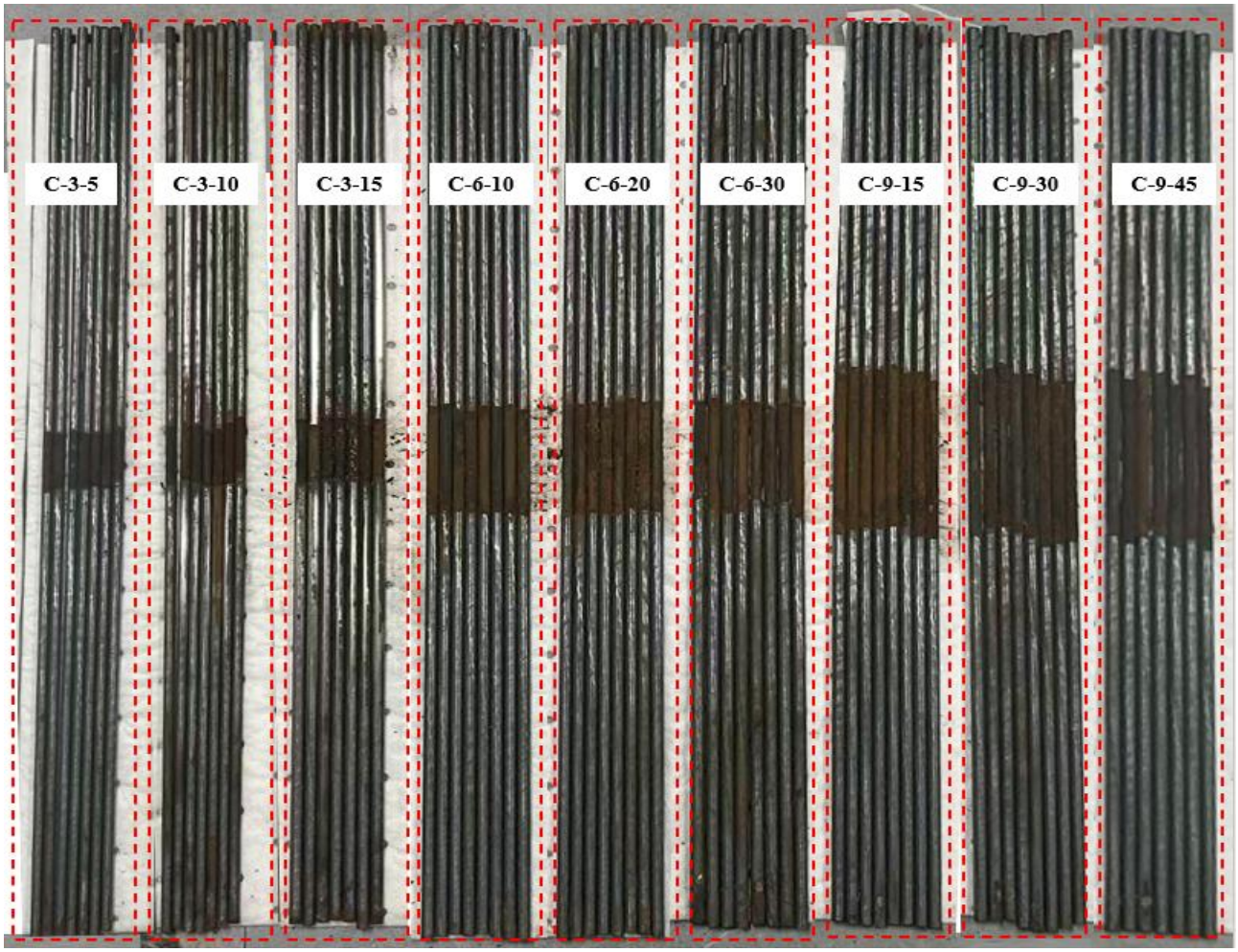

Figure 5: Appearance of uniformly corroded steel wire

3. Corrosion Damage Simulation

3.1 Simulation Model Parameter Settings

To investigate the detection of corrosion damage in cable-stayed bridges, this study employed COMSOL Multiphysics simulation software to model corroded cables. Uniform corrosion damage

was simulated using Boolean difference set theory, with hollow cylinders representing the corrosion layer. The severity of corrosion damage was controlled by adjusting the cylinder thickness. The complete simulation model is illustrated in Figure 6.

First, establish a 3D model using the built-in 3D modeling function of the software, primarily including steel cables, lightweight differential electromagnetic sensors, air domains, and infinite source domains. Relevant parametric variables are defined to control the corrosion extent of the cable-stayed structure, and a combined tetrahedral mesh and boundary layer mesh approach is employed for meshing.

Secondly, material properties were defined. The steel wire in the corrosion-damaged section of the cable was severely damaged, and air material was used for simulation. The material configuration of the lightweight differential electromagnetic sensor coil and steel cable is shown in Table 2.

Finally, add the research content. Step 1 steady-state study and Step 2 parameterized scanning are included, with a parameter value list configured. Through parameter scanning configuration, damage sites are detected, and the induced voltage of the lightweight electromagnetic differential sensor is extracted for data analysis in simulation results.

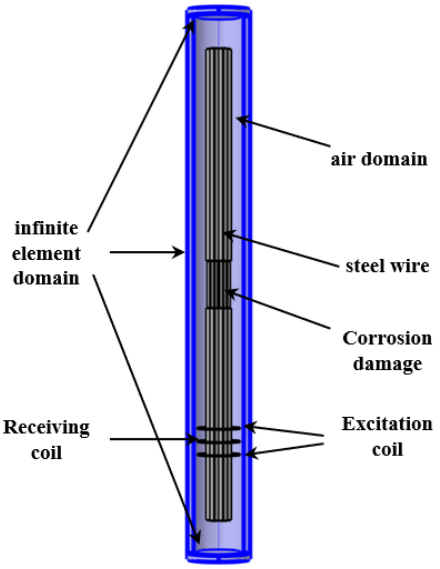

Figure 6: Overall simulation model diagram

Table 2: Parameters of specimens and coils

Material	relative permeability	electrical conductivity (S/m)	constant-pressure heat capacity(J/(kg*K))	density (kg/m^3)
Structural steel	40	4.032e6	475	7850
Copper	1	5.998e7	385	8960

3.2 Simulation Result Analysis

Based on the simulation model established in Section 3.1, this study investigates the effects of varying corrosion severity and width on detection signals in lightweight differential electromagnetic sensors. Metal loss rates were $R_s$set at 10%,20%,30%, and 40%, with corrosion widths configured at 30,60, and 90 mm. The simulation results are presented in Figure 7, which displays the

characteristic parameter of mutual inductance between the excitation coil and receiving coil, reflecting the ratio of induced voltage to excitation current. This parameter is utilized to characterize the detection signals.

The simulation detection curves shown in Figure 7(a-g) demonstrate that under specified corrosion severity and width parameters, signal spikes consistently occur when the sensor reaches the cable's corrosion damage location during the simulation process. These results confirm that the lightweight differential electromagnetic sensor employing eddy current testing technology can effectively detect uniform corrosion damage in cable structures under simulated conditions, thereby validating its feasibility for corrosion damage detection applications.

Analysis of the simulation curve patterns reveals distinct characteristics in how corrosion width and severity affect detection curves. Figures 7(a-c) demonstrate detection curves under varying corrosion conditions. When corrosion width remains constant, increasing corrosion severity leads to progressively greater abrupt changes in damage zone detection curves, with more pronounced signal amplitude variations while peak-to-peak spacing at transition points shows no significant fluctuations. Figures 7(d-g) present curves with varying corrosion widths. When corrosion severity remains unchanged, altering only corrosion width results in minimal changes to detection curve abruptness, while peak-to-peak spacing at transition points continues to increase with wider corrosion widths.

The above rules show that the peak-to-peak size of the detection curve is a response to the degree of corrosion, and the peak-to-peak spacing of the detection curve reflects the change of the corrosion width. This conclusion provides theoretical support for the detection of the corrosion damage of the cable based on the eddy current detection principle of the lightweight differential electromagnetic sensor.

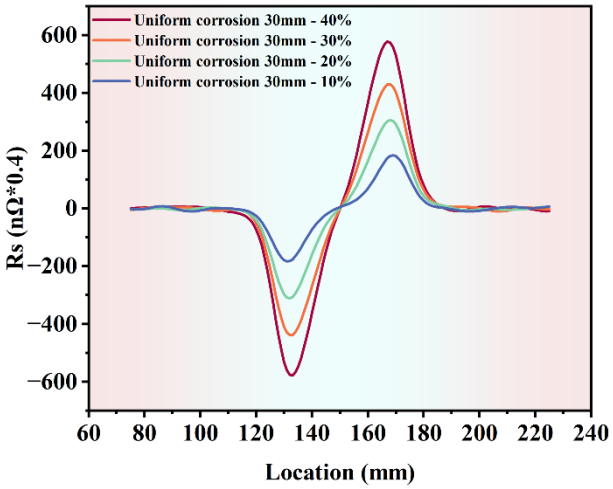

(a) Detection curves of different corrosion degrees with a corrosion width of 30 mm

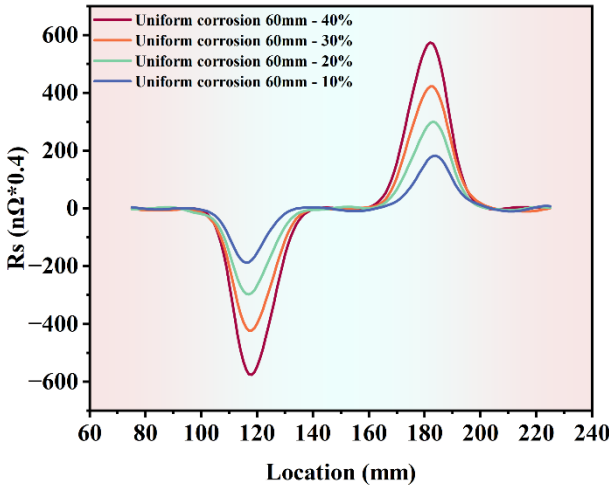

(b) Detection curves of different corrosion degrees with a corrosion width of 60 mm

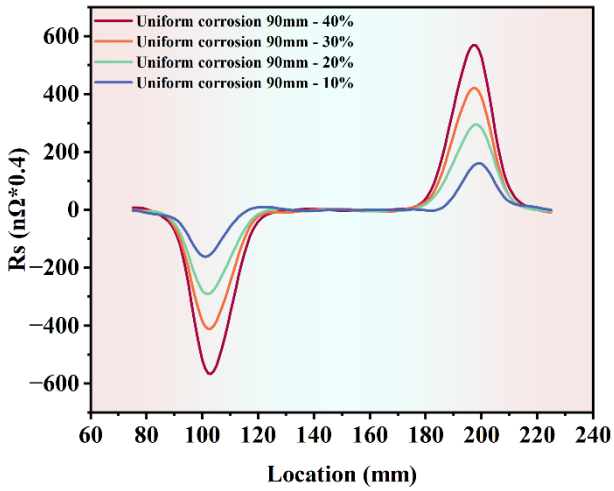

(c) Detection curves of different corrosion degrees with a corrosion width of 90 mm

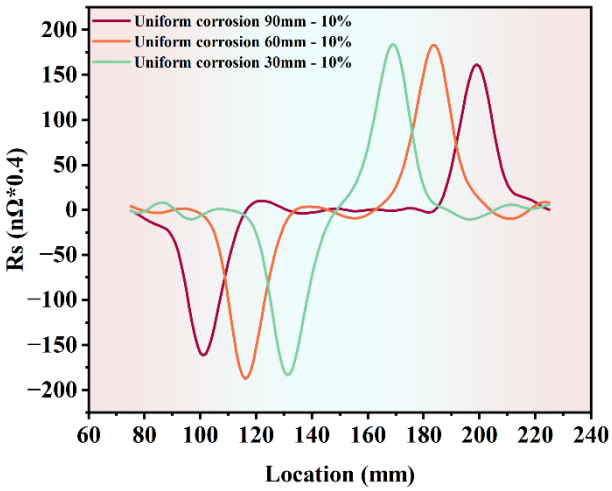

(d) Detection curves of different corrosion widths with a corrosion degree of 10%

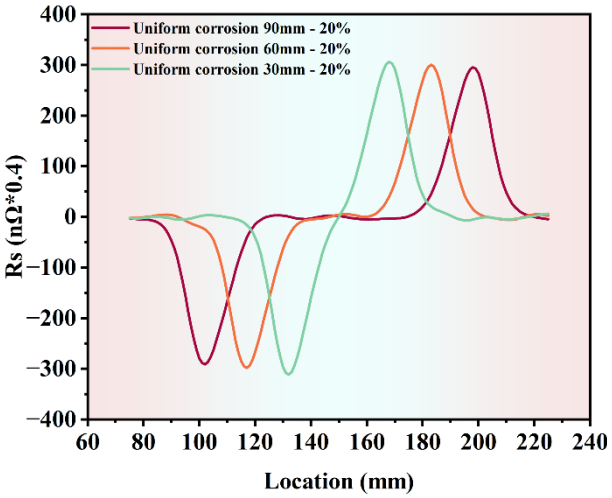

(e) Detection curves of different corrosion widths with a corrosion degree of 20%

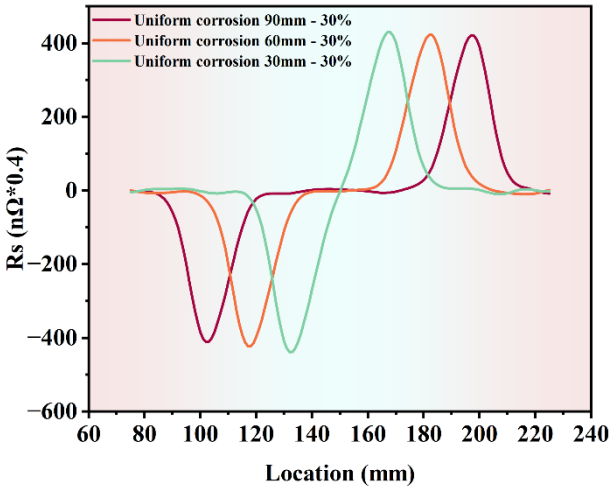

(f) Detection curves of different corrosion widths with a corrosion degree of 30%

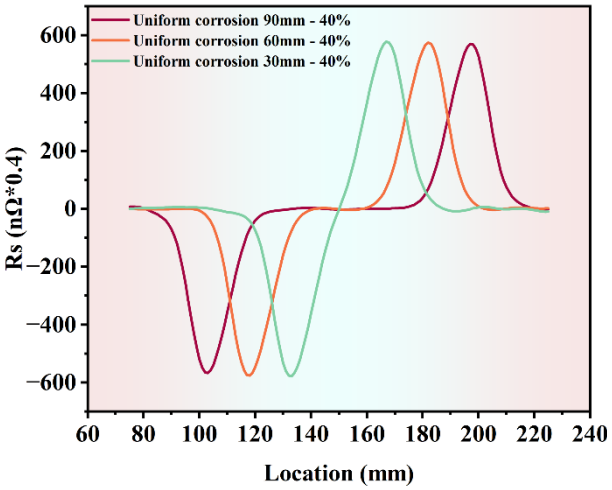

(g) Detection curves of different corrosion widths with a corrosion degree of 40%

Figure 7. Simulation detection curve diagram

4. Analysis of Experimental Results

4.1 Analysis of pitting damage test results

To investigate the impact of different pitting corrosion damage on detection signals, pitting corrosion specimens with hemispherical notches were tested, featuring notch depths of 1mm, 2mm, and 3mm, and notch lengths of 2mm, 4mm, and 6mm in sequence. Figure 8 displays detection signal patterns of pitting corrosion damage on cable-stayed bridges. When lightweight differential sensors encounter pitting corrosion damage, detection signals exhibit significant abrupt changes with mutation intensity far exceeding environmental interference. Specimens with varying pitting severity all demonstrate pronounced signal fluctuations at damaged locations, which intensify progressively with increasing pitting depth. These findings confirm that lightweight differential electromagnetic sensors based on eddy current detection principles possess effective capability for detecting pitting corrosion damage in cable-stayed bridges. The correlation between mutation intensity and pitting severity provides a novel approach for corrosion damage detection in cable-stayed structures.

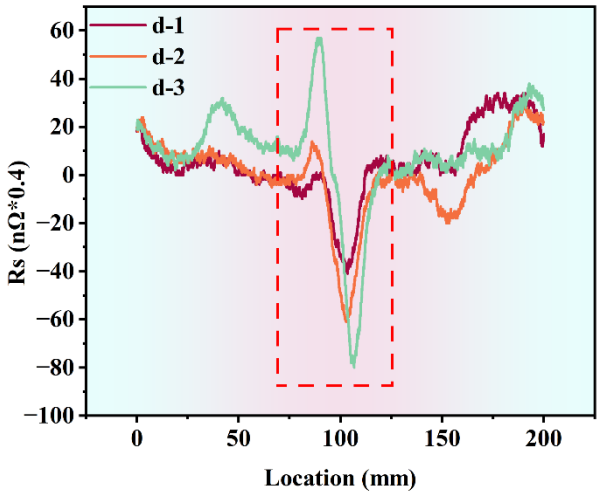

Figure 8. Detection signal diagrams of stay cables with different pitting corrosion damages

4.2 Analysis of Uniform Corrosion Damage Test Results

4.2.1 Correlation Analysis between Corrosion Severity and Detection Signals

To investigate the impact of varying degrees of uniform corrosion damage on detection signals, specimens with different corrosion levels were tested. All other variables were kept consistent except for the corrosion severity to ensure scientific validity and comparability of experimental results. Figures 9(a-c) show detection signal patterns of cables with different levels of uniform corrosion damage. All experimental data in the figures represent the average values from three repeated experiments. When lightweight differential sensors undergo uniform damage, the detection signals exhibit significant abrupt changes. As corrosion intensifies, the peak-to-peak amplitude of the signals increases, while the peak-to-peak spacing remains relatively stable. The results demonstrate that the sensor can effectively detect uniform corrosion damage in cables, with the peak-to-peak amplitude showing a correlation with corrosion severity. This detection phenomenon aligns well with simulation conclusions, providing a new approach for cable damage prevention and corrosion assessment.

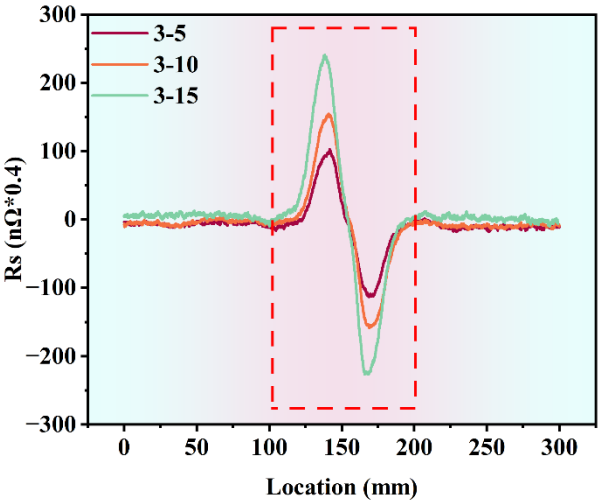

(a) Detection curves for different corrosion degrees at a corrosion width of 30 mm

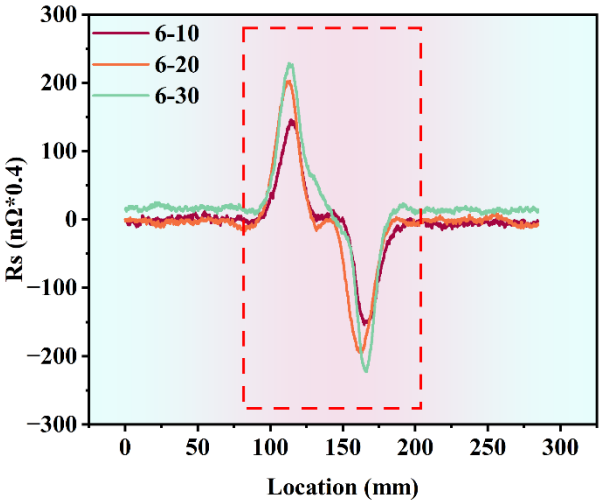

(b) Detection curves for different corrosion degrees at a corrosion width of 60 mm

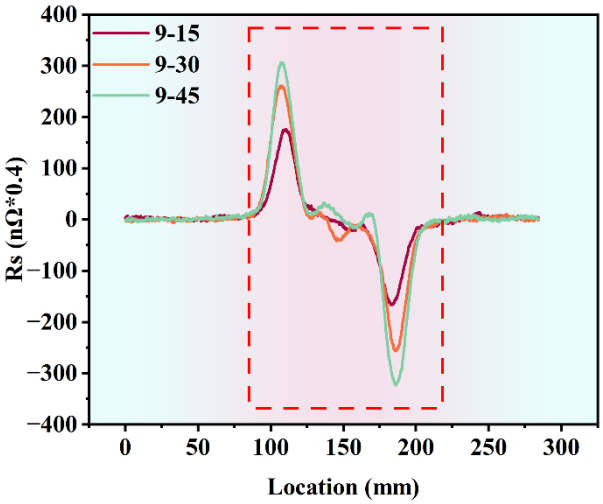

(c)Detection curves for different corrosion degrees at a corrosion width of 90 mm

Figure 9. Detection signal diagrams of stay cables with different degrees of uniform corrosion damage

4.2.2 Correlation Analysis between Corrosion Width and Detection Signals

To investigate the impact of varying corrosion widths on detection signals from uniform corrosion damage, specimens with different corrosion widths were tested. All other variables were kept consistent except for the corrosion width to ensure scientific validity and comparability of experimental results. Figures 10(a-c) show detection signal patterns of cables with uniform corrosion damage at different widths. All experimental data in the figures represent average values from three repeated experiments. The results demonstrate that when lightweight differential sensors undergo uniform corrosion damage, their detection signals exhibit significant abrupt changes. As the corrosion width increases, the peak-to-peak amplitude of the detection signal shows no significant regular variation, with fluctuations remaining within reasonable error ranges. However, the peak-to-peak spacing gradually increases, and the mutation interval expands proportionally with corrosion width. These findings indicate a correlation between peak-to-peak spacing and corrosion width in cable detection signals. This observation aligns well with simulation conclusions,

validating the established pattern and providing a new approach for damage prevention and corrosion width assessment in cable systems.

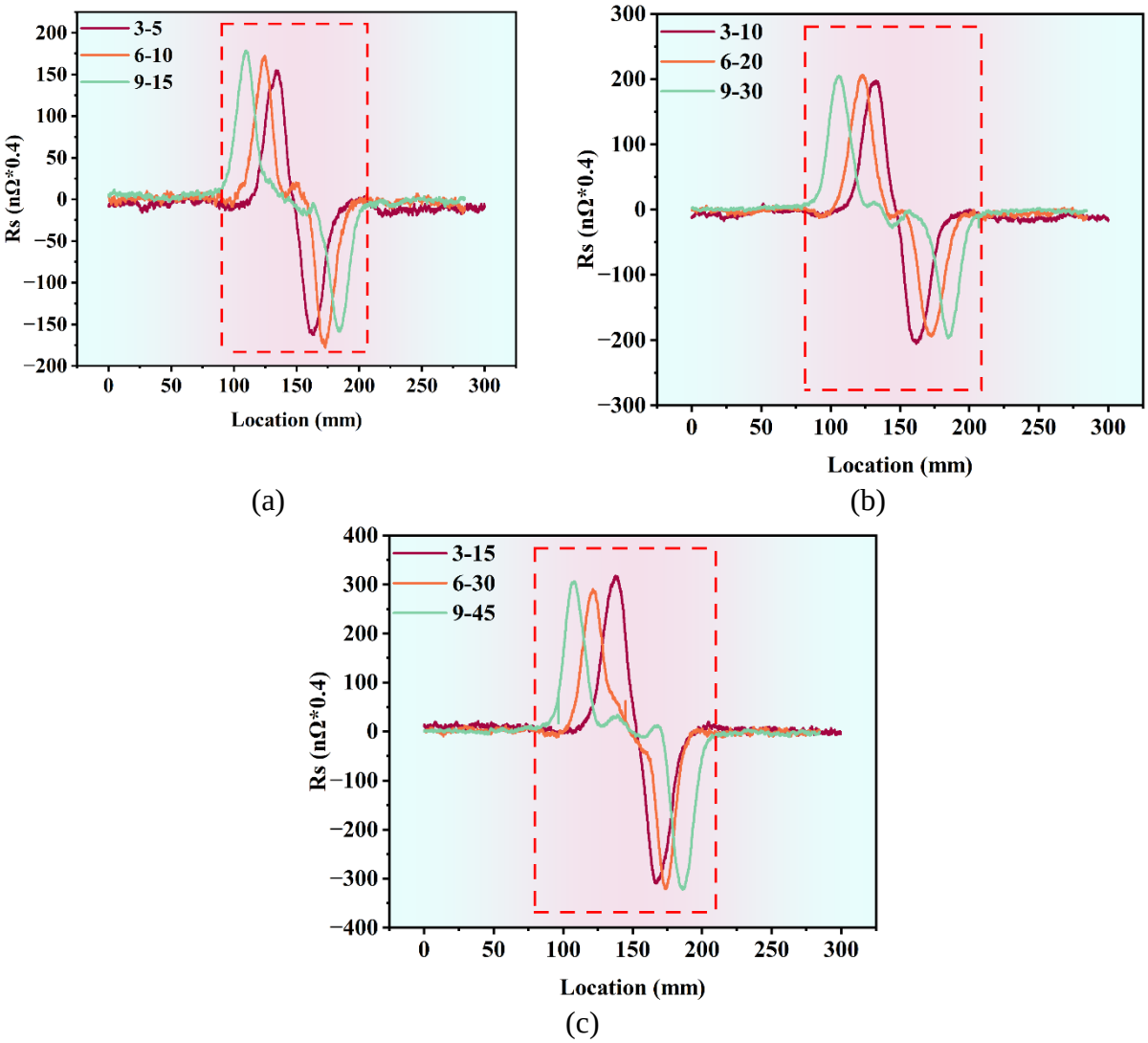

Figure 10. Detection signal diagrams of stay cables with different degrees of uniform corrosion damage

5. Conclusion

This study conducts systematic research on corrosion damage detection for cable-stayed bridges, employing a lightweight differential electromagnetic sensor based on eddy current testing principles as the core detection tool. By integrating experimental and simulation methods, we validate the feasibility of this sensor in detecting corrosion damage on cable-stayed structures and analyze the impact patterns of corrosion parameters on detection signals.

To investigate two typical engineering corrosion forms-pitting corrosion and uniform corrosion-we developed high-quality experimental specimens. Pitting corrosion specimens were fabricated through mechanical cutting to ensure geometric consistency, while uniform corrosion specimens underwent electrochemical accelerated corrosion using a custom-designed multi-wire series electrolytic cell, significantly improving preparation efficiency and rust layer uniformity to provide reliable experimental data for subsequent analysis. Based on COMSOL Multiphysics

simulation software, we established a corrosion damage detection model for cable-stayed bridges, employing Boolean difference set methodology to simulate uniform corrosion damage. Simulation results demonstrated that under constant corrosion severity conditions, the peak-to-peak spacing at detection signal abrupt changes increased substantially with corrosion width progression. Conversely, when corrosion width remained constant, signal mutation intensity escalated with worsening corrosion severity. Experimental verification showed excellent agreement with simulation patterns. When sensors passed through corrosion-defective areas, distinct waveform transitions were observed, further validating the sensor's feasibility and effectiveness in corrosion damage detection for cable-stayed structures. These findings provide scientific foundations and technical support for engineering applications in corrosion damage assessment of cable-stayed bridges.

References

[1] Ding Y, Ye X W, Su Y H, et al. A framework of cable wire failure mode deduction based on Bayesian network[J]. Structures, 2023, 57: 104996.

[2] Yang Z, Wang C, Li Y, et al. Finite element-based data-driven method to detect multiple damages of 1D beam model and 2D slab model of bridges-A theoretical and experimental study[J]. Measurement, 2025, 241: 115709.

[3] Sun L, Chen L, Huang H. Stay cable vibration mitigation: A review[J]. Advances in Structural Engineering, 2022, 25(16): 3368-3404.

[4] Sousa Tomé E, Pimentel M, Figueiras J. Structural response of a concrete cable-stayed bridge under thermal loads[J]. Engineering Structures, 2018, 176: 652-672.

[5] Ho H N, Kim K D, Park Y S, et al. An efficient image-based damage detection for cable surface in cable-stayed bridges[J]. NDT & E International, 2013, 58: 18-23.

[6] Gao D, Chen W L, Zhang R T, et al. Multi-modal vortex- and rain-wind- induced vibrations of an inclined flexible cable[J]. Mechanical Systems and Signal Processing, 2019, 118: 245-258.

[7] Yao G, Zeng G, He X, et al. Study on corrosion damage mechanisms and fatigue life of corroded steel wires in suspension bridge cable strands[J]. Case Studies in Construction Materials, 2025, 23: e05042.

[8] Yuan Y, Liu X, Pu G, et al. Temporal and spatial variability of corrosion of high-strength steel wires within a bridge stay cable[J]. Construction and Building Materials, 2021, 308: 125108.

[9] Cukaci C E, Soyoz S. Cable tension estimation of cable-stayed bridge using vision-based modal identification[J]. Procedia Structural Integrity, 2024, 64: 531-538.

[10] Li D L, Yang D H, Yi T H, et al. Anomaly diagnosis of stay cables based on vehicle-induced cable force sums[J]. Engineering Structures, 2023, 289: 116239.

[11] Li S, Wei S, Bao Y, et al. Condition assessment of cables by pattern recognition of vehicle-induced cable tension ratio[J]. Engineering Structures, 2018, 155: 1-15.

[12] Wang B, Wang D, Chong H, et al. Detection and quantitative characterization of dynamic contact states of bending tribo-corrosion-fatigue steel wire ropes[J]. Tribology International, 2026, 215: 111480.

[13] Liu S, Sun Y, Jiang X, et al. A new MFL imaging and quantitative nondestructive evaluation method in wire rope defect detection[J]. Mechanical Systems and Signal Processing, 2022, 163: 108156.

[14] Djeddi L, Khelif R, Benmedakhene S, et al. Reliability of Acoustic Emission as a Technique to Detect Corrosion and Stress Corrosion Cracking on Prestressing Steel Strands[J]. International Journal of Electrochemical Science, 2013, 8(6): 8356-8370.

[15] Vanniamparambil A P ,Khan F ,Hazeli K , et al. Novel optico-acoustic nondestructive testing for wire break detection in cables[J].Structural Control and Health Monitoring,2013,20(11):1339-1350.DOI:10.1002/stc.1539.

[16] Zhang B, Luo Z, Hong X, et al. Deep learning-based corrosion-like defect localization technique for high-voltage cable aluminum sheaths using guided waves[J]. Measurement Science and Technology, 2023, 34(8): 084006.

[17] Seo D, Kim J, Park S. An Experimental Study on Defect Detection of Anchor Bolts Using Non-Destructive Testing Techniques.[J]. Materials, 2023, 16(13): 4861.

[18] Zitoun A, Dixon S, Kazilas M, et al. Defect Detection and Imaging in Composite Structures Using Magnetostrictive Patch Transducers[J]. Sensors, 2023, 23(2): 600.

[19] Wu D, Liu Z, Wang X, et al. Composite magnetic flux leakage detection method for pipelines using alternating magnetic field excitation[J]. NDT & E International, 2017, 91: 148-155.